nature physics

SUPPLEMENTARY INFORMATION

DOI: 10.1038/NPHYS2524

Electrical tuning of valley magnetic moment through symmetry control in bilayer MoS_2

Sanfeng Wu[1], Jason S Ross[2], Gui-Bin Liu[3], Grant Aivazian[1], Aaron Jones[1], Zaiyao Fei[1], Wenguang Zhu[4-6], Di Xiao[4,7], Wang Yao[3], David Cobden[1], Xiaodong Xu[1,2†]

[†]Email: xuxd@uw.edu

Table of Contents:

S1. Polarization of bilayer devices at zero gate voltage

S2. Initial electron doping effect on bilayer devices

S3. Photoluminescence intensity as a function of gate voltage

S4. Ab initio Density Functional Theory Calculation

S5. Tight Banding Calculation of Orbital Magnetic Moment

S6. Supplemental References

DOI: 10.1038/NPHYS2524

S1. Polarization of bilayer devices at zero gate voltage

Device #	B1	B2	B3	B4	B5	B6	B7	B8	B9
η	31%	14%	12%	20%	16%	30%	17%	28%	16%

Table S1: We have measured a number of bilayer devices and all exhibit a nonzero degree of photoluminescence (PL) polarization (10% ~ 30%) at zero gate voltage. This observation indicates the existence of inversion symmetry breaking in bilayer MoS_2. The exact mechanism causing the inversion asymmetry is unclear but it is likely from the coupling to the substrates[1], consistent with the initial electron doping effect described in section **S2**.

S2. Initial Electron Doping Effect on Bilayer Devices

In the main text, we show that PL polarization vanishes around V_g = -60 V for device B2, where the top and bottom layers reach equal potential. Since the negative gate voltage depletes electrons or induces hole doping, the devices are initially electron doped as previous reported[2]. All measured devices show the same trend for η to decrease as V_g decreases from positive to negative, consistent with initial electron doping; however, initial doping varies between devices. Figure S1 shows the degree of PL polarization from two devices under right-hand circularly polarized light excitation. Due to the electron doping in these devices, the critical voltage for vanishing PL polarization is out of the accessible voltage range (beyond -100 V).

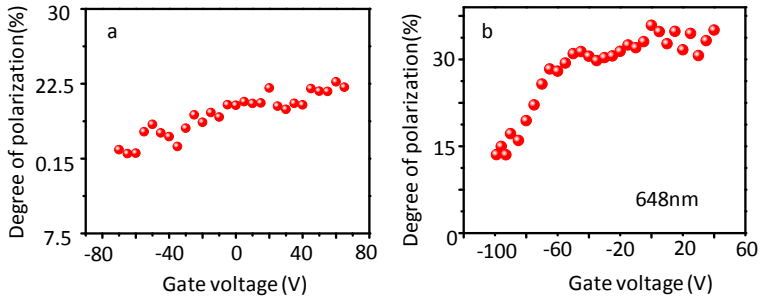

Figure S1| Degree of PL polarization under right-hand circularly polarized light excitation as a function of gate voltage from **a**, device B4 and **b**, device B9.

S3. Photoluminescence as a Function of Gate Voltage

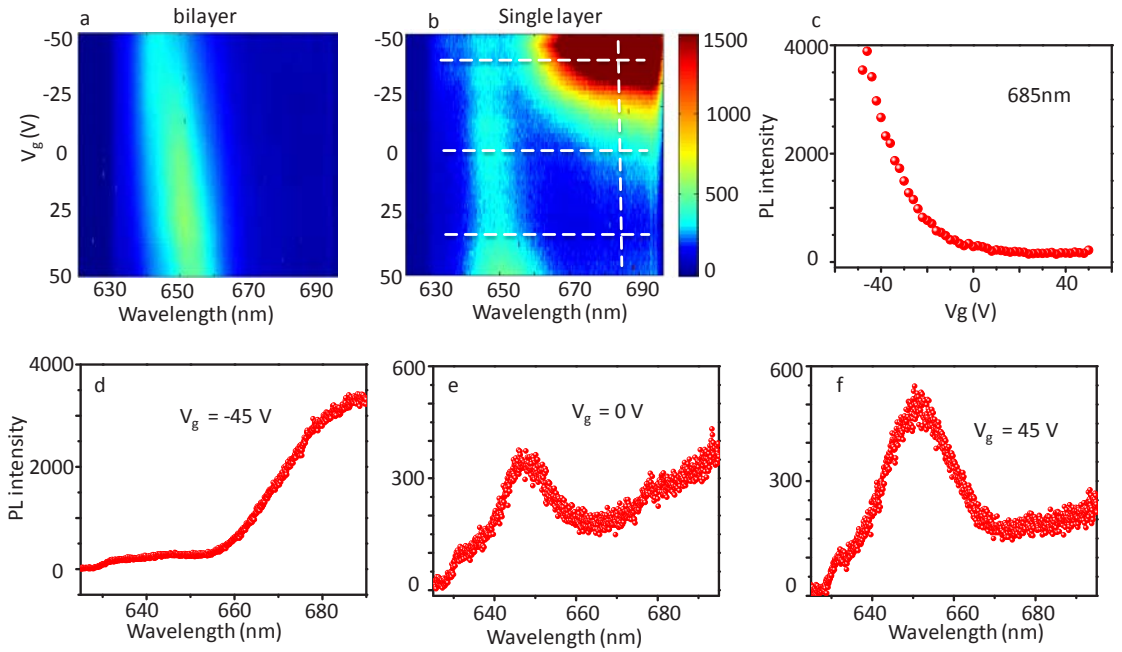

Figure S2| PL intensity as a function of gate voltage under 532 nm light excitation. CCD exposure time: 15 seconds. **a**, PL intensity map of bilayer MoS_2 as a function of wavelength and gate voltage. **b**, PL intensity map of monolayer MoS_2. As shown in c-f, the PL intensity from the impurity peak has a strong V_g dependence. These traces are extracted from the dashed lines in b. **c,** PL intensity at 685 nm vs. V_g. The data show that the PL intensity from the impurity peak decreases drastically as the chemical potential increases. PL spectrum at **d**, V_g = -45 V, **e**, V_g = 0 V, and **f,** V_g = 45 V.

S4. Ab initio Density Functional Theory Calculation

Our first-principles density functional theory calculations were carried out using the projector augmented wave (PAW) method[3-4] with the local density approximation (LDA)[5] for exchange correlation as implemented in the Vienna Ab Initio Simulation Package (VASP)[6]. The Mo(4p,4d,5s) and S(3s,3p) electrons were treated as valence. A plane-wave energy cutoff of 600.0 eV was consistently used and a total of 80 bands were included in all the calculations. The supercell contains a 1×1 unit cell of MoS_2 bilayer and a vacuum region of 16 Å. A 36×36×1 special **k**-point mesh including the Γ point was used for integration over the Brillouin zone. Optimized atomic structures were achieved when forces on all the atoms were smaller than 0.001eV/Å. The optimized crystal parameter is 3.13 Å for MoS_2 bilayer. To generate a perpendicular external electric field, an artificial dipole layer was placed in the middle of the

DOI: 10.1038/NPHYS2524

vacuum region [7].

S5. Tight Banding (TB) Calculation of Orbital Magnetic Moment

In AB stacked MoS_2 bilayer, the top layer can be obtained by rotating the bottom layer by 180 degrees and then moving it up such that S atoms of the top layer sit on top of Mo atoms of the bottom layer and vice versa (See Fig. 1 in the main text). The effective Hamiltonian of MoS_2 bilayer therefore can be constructed from that of MoS_2 single layer, given in Ref. 8. Taking into account the point group symmetry D_{3d} of MoS_2 bilayer, a linearized TB Hamiltonian in the neighborhood of $\pm K$ points is obtained as

$$H_0(\mathbf{k}) = \begin{bmatrix} \Delta & at(\tau k_x + ik_y) & 0 & 0 \\ at(\tau k_x - ik_y) & -\Delta & 0 & r \\ 0 & 0 & \Delta & at(\tau k_x - ik_y) \\ 0 & r & at(\tau k_x + ik_y) & -\Delta \end{bmatrix} \qquad (1.1)$$

where 2Δ is the band gap of MoS_2 single layer, a is the lattice constant, t is the effective in-plane hopping integral, r is the effective interlayer interaction, and $\tau = \pm 1$ is the valley index. The diagonal blocks are the same as the single layer Hamiltonian. The particular form of the off-diagonal block, which represents the inter-layer coupling, is determined by the D_{3d} symmetry. The basis of $H_0(\mathbf{k})$ are

$$|\psi_1\rangle = |d^{\mathrm{t}}_{z^2}\rangle, \quad |\psi_2^\tau\rangle = \frac{1}{\sqrt{2}}(-i\tau|d^{\mathrm{t}}_{xy}\rangle + |d^{\mathrm{t}}_{x^2-y^2}\rangle), \quad |\psi_3\rangle = |d^{\mathrm{b}}_{z^2}\rangle, \quad |\psi_4^\tau\rangle = \frac{1}{\sqrt{2}}(i\tau|d^{\mathrm{b}}_{xy}\rangle + |d^{\mathrm{b}}_{x^2-y^2}\rangle) \qquad (1.2)$$

where the superscript t and b stands for the "top" and "bottom" layers, respectively.

An applied gate electric field introduces a potential difference $2V$ between the two layers. The effective Hamiltonian becomes

$$H(\mathbf{k}) = \begin{bmatrix} \Delta + V & at(\tau k_x + ik_y) & 0 & 0 \\ at(\tau k_x - ik_y) & -\Delta + V & 0 & r \\ 0 & 0 & \Delta - V & at(\tau k_x - ik_y) \\ 0 & r & at(\tau k_x + ik_y) & -\Delta - V \end{bmatrix} \qquad (1.3)$$

The parameters are taken as $a = 3.193\,\text{Å}$, $\Delta = 0.83$ eV, $t = 1.10$ eV, $r = 0.047$ eV.

The orbital magnetic moment $\mathbf{M}_n(\mathbf{k})$ and Berry curvature $\Omega_n(\mathbf{k})$ for Bloch electrons are defined respectively[9-10] by

$$\mathbf{M}_n(\mathbf{k}) = -i\frac{e}{\hbar}\langle\nabla_{\mathbf{k}}u_n|\times(H-\varepsilon_n)|\nabla_{\mathbf{k}}u_n\rangle \qquad (1.4)$$

$$\Omega_n(\mathbf{k}) = i\langle\nabla_{\mathbf{k}}u_n|\times|\nabla_{\mathbf{k}}u_n\rangle \qquad (1.5)$$

where u_n is the periodical part of Bloch state and ε_n is the nth band energy of Bloch state. In the

experiment, the incident photons only excite the lowest energy transition near the K points. Then the relevant orbital magnetic moments and Berry curvatures are from the top most valance band at $\pm K$ points (all are z components due to 2D system). Under the condition, $r, V \ll \Delta$, we obtain

$$m = \frac{\tau e a^2 t^2}{2\hbar\Delta} \frac{V}{\sqrt{r^2 + V^2}}. \qquad (1.6)$$

$$\Omega = -\frac{\tau a^2 t^2}{2\Delta^2} \frac{V}{\sqrt{r^2 + V^2}} = -\frac{\hbar}{\Delta e} \mathrm{m} \qquad (1.7)$$

S6. Supplementary References

1 Kin Fai Mak, Keliang He, Jie Shan & Heinz, T. F. Control of valley polarization in monolayer MoS2 by optical helicity. *Nature Nanotechnology, doi:10.1038/nnano.2012.96* (2012).

2 RadisavljevicB, RadenovicA, BrivioJ, GiacomettiV & KisA. Single-layer MoS2 transistors. *Nat Nano* **6**, 147-150 (2011).

3 Kresse, G. & Furthmüller, J. Efficient iterative schemes for ab initio total-energy calculations using a plane-wave basis set. *Physical Review B* **54**, 11169-11186 (1996).

4 Blöchl, P. E. Projector augmented-wave method. *Physical Review B* **50**, 17953-17979 (1994).

5 Perdew, J. P. & Zunger, A. Self-interaction correction to density-functional approximations for many-electron systems. *Physical Review B* **23**, 5048-5079 (1981).

6 Kresse, G. & Joubert, D. From ultrasoft pseudopotentials to the projector augmented-wave method. *Physical Review B* **59**, 1758-1775 (1999).

7 Makov, G. & Payne, M. C. Periodic boundary conditions in ab initio calculations. *Physical Review B* **51**, 4014-4022 (1995).

8 Xiao, D., Liu, G.-B., Feng, W., Xu, X. & Yao, W. Coupled Spin and Valley Physics in Monolayers of MoS_2 and Other Group-VI Dichalcogenides. *Physical Review Letters* **108**, 196802 (2012).

9 Chang, M.-C. & Niu, Q. Berry phase, hyperorbits, and the Hofstadter spectrum: Semiclassical dynamics in magnetic Bloch bands. *Physical Review B* **53**, 7010-7023 (1996).

10 Xiao, D., Chang, M.-C. & Niu, Q. Berry phase effects on electronic properties. *Reviews of Modern Physics* **82**, 1959-2007 (2010).